UC Davis
UC Davis Previously Published Works

Title

Tree growth acceleration and expansion of alpine forests: The synergistic effect of atmospheric and edaphic change

Permalink

Journal

ISSN

Authors

Silva, Lucas CR
Sun, Geng
Zhu-Barker, Xia
et al.

Publication Date

DOI

Peer reviewed

PLANT SCIENCES

Tree growth acceleration and expansion of alpine forests: The synergistic effect of atmospheric and edaphic change

Lucas C. R. Silva,[1] Geng Sun,[2]* Xia Zhu-Barker,[3] Qianlong Liang,[4] Ning Wu,[2] William R. Horwath[3]

Many forest ecosystems have experienced recent declines in productivity; however, in some alpine regions, tree growth and forest expansion are increasing at marked rates. Dendrochronological analyses at the upper limit of alpine forests in the Tibetan Plateau show a steady increase in tree growth since the early 1900s, which intensified during the 1930s and 1960s, and have reached unprecedented levels since 1760. This recent growth acceleration was observed in small/young and large/old trees and coincided with the establishment of trees outside the forest range, reflecting a connection between the physiological performance of dominant species and shifts in forest distribution. Measurements of stable isotopes (carbon, oxygen, and nitrogen) in tree rings indicate that tree growth has been stimulated by the synergistic effect of rising atmospheric CO_2 and a warming-induced increase in water and nutrient availability from thawing permafrost. These findings illustrate the importance of considering soil-plant-atmosphere interactions to understand current and anticipate future changes in productivity and distribution of forest ecosystems.

INTRODUCTION

Recent alterations in atmospheric composition and climate have profoundly affected the performance of plant species, causing shifts in ecosystem distribution across biomes (*1*–*3*). A long tradition of research in controlled environments supports the notion that plant productivity and resource-use efficiency, particularly of tree species, are stimulated under CO_2 enrichment (*4*). However, in natural forest ecosystems, rising atmospheric CO_2 concentration has seldom translated into increased tree growth, an observation that is generally attributed to water and/or nutrient limitation (*5*–*8*).

Globally, soil nutrient and water availability are key regulators of ecosystem productivity (*2*, *9*). Under nonlimiting conditions, the response of trees and, by extension, forests to elevated CO_2 should be positive (*10*), but at the individual and ecosystem scales, productivity declines when soil resources become limiting. This is evident in the strong association between soil fertility and foliar assimilation of carbon and nitrogen (*11*, *12*) and in the progressive nutrient limitation that follows an initial CO_2 stimulation of forest growth (*13*). Tree ring records generally provide limited support for a CO_2 "fertilization" of forest biomes (*7*). However, in some alpine ecosystems, the combined effect of climate warming and rising CO_2 levels has been shown to enhance the productivity of dominant trees (*14*–*16*), which could lead to forest expansion. Investigating the mechanisms behind such response is the objective of this study.

On the basis of anticipated connections between physiological, ecological, and biogeochemical drivers of vegetation dynamics (*17*), we hypothesized that synergies between fast processes (for example, plant resource use and photosynthesis) and slow processes (for ex-

ample, species migration and soil development) control how ecosystems respond to changes in climate and atmospheric composition. Specifically, we expected to find concurrent shifts in tree growth and forest distribution in alpine ecotones, triggered by rising temperatures and atmospheric CO_2 concentration and modulated by spatial and temporal variation in the availability of soil resources. To test this hypothesis, we characterized a vegetation gradient in eastern Tibet, spanning forests, forest patches, and isolated trees growing in open grasslands (Fig. 1 and fig. S1). In each of these habitats, we sampled dominant *Abies faxoniana* trees and combined dendrochronological and isotopic measurements to examine changes in tree growth, resource use, and time of establishment over the past ~250 years.

RESULTS

Tree growth acceleration

We identified a recent surge in tree growth for all trees across the gradient. Steady, but very low, basal area increments (BAI) were observed between the 1760s and the early 1900s (5 cm^2 year^{-1}). Marked increases in BAI during the 1930s and then again in the 1960s (>15 cm^2 year^{-1}) led to accelerated growth in recent years (20 to 30 cm^2 year^{-1}; Fig. 2). At the sampling event, tree age and size varied considerably across the gradient (7- to 32-cm radius and 40 to 250 years; fig. S2). The smallest/youngest trees were sampled in open grasslands, where their ingress (~60 years ago) coincided with the increase in growth of the largest/oldest trees in the forest interior (Fig. 2). Growth rates varied with cambial age and tree size. Small/young trees have grown faster than large/old trees (table S1 and Fig. 2), but all trees showed a rapid increase in growth over the past century, coinciding with rising temperatures and atmospheric CO_2 levels (tables S2 and S3). Age-related changes in ring width were nonlinear, with divergent trends observed across the gradient (Fig. 3). Once ontogenic effects were removed, normalized ring widths confirmed a steady increase in tree growth with calendar year (Fig. 3). The analysis of ring widths and

[1]Environmental Studies Program and Department of Geography, University of Oregon, Eugene, OR 97403, USA. [2]Key Laboratory of Mountain Ecological Restoration and Bioresource Utilization, Ecological Restoration Biodiversity Conservation Key Laboratory of Sichuan Province, Chengdu Institute of Biology, Chinese Academy of Sciences, Sichuan 610041, China. [3]Department of Land, Air, and Water Resources, University of California, Davis, CA 95616, USA. [4]College of Life Science, Sichuan University, Sichuan 610041, China.
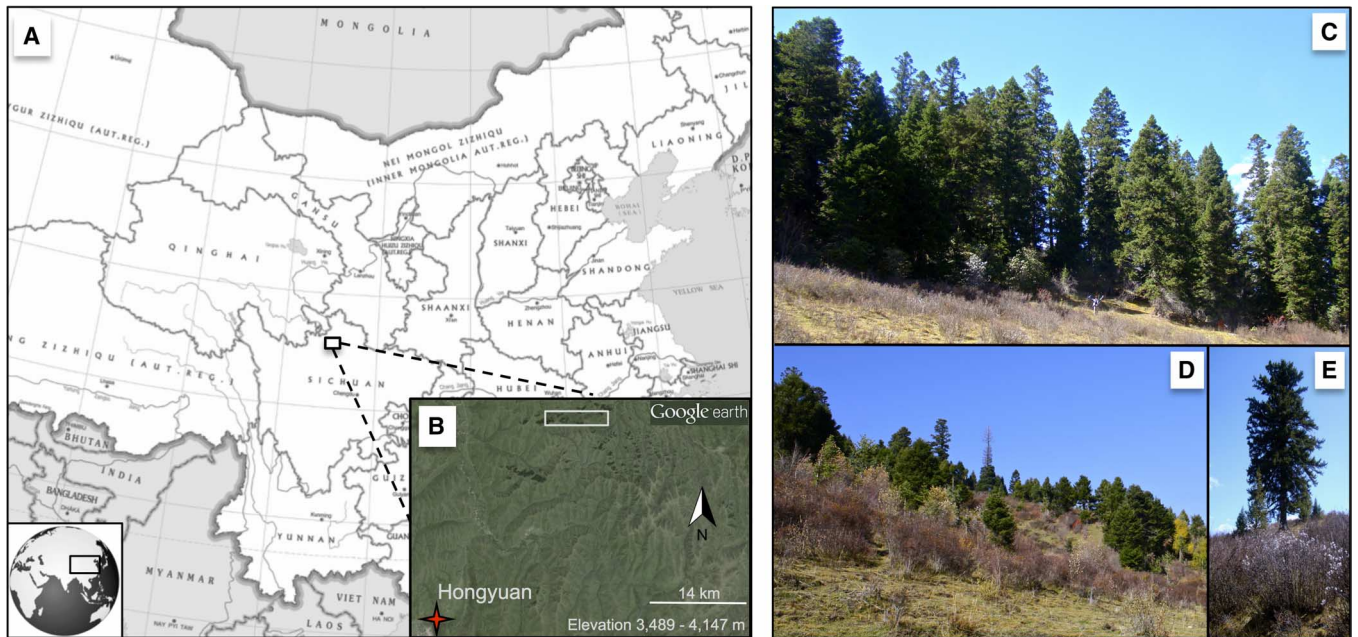*Corresponding author. Email: sungeng@cib.ac.cn

Fig. 1. Study site. (**A**) Map of the region. (**B**) Location of study site and Hongyuan County meteorological station. (**C**) Forest-grassland border. (**D**) Small forest patches. (**E**) Isolated tree. Map source: Chinese Bureau of Surveying and Mapping and Google Earth. Photo credit: L. Silva.
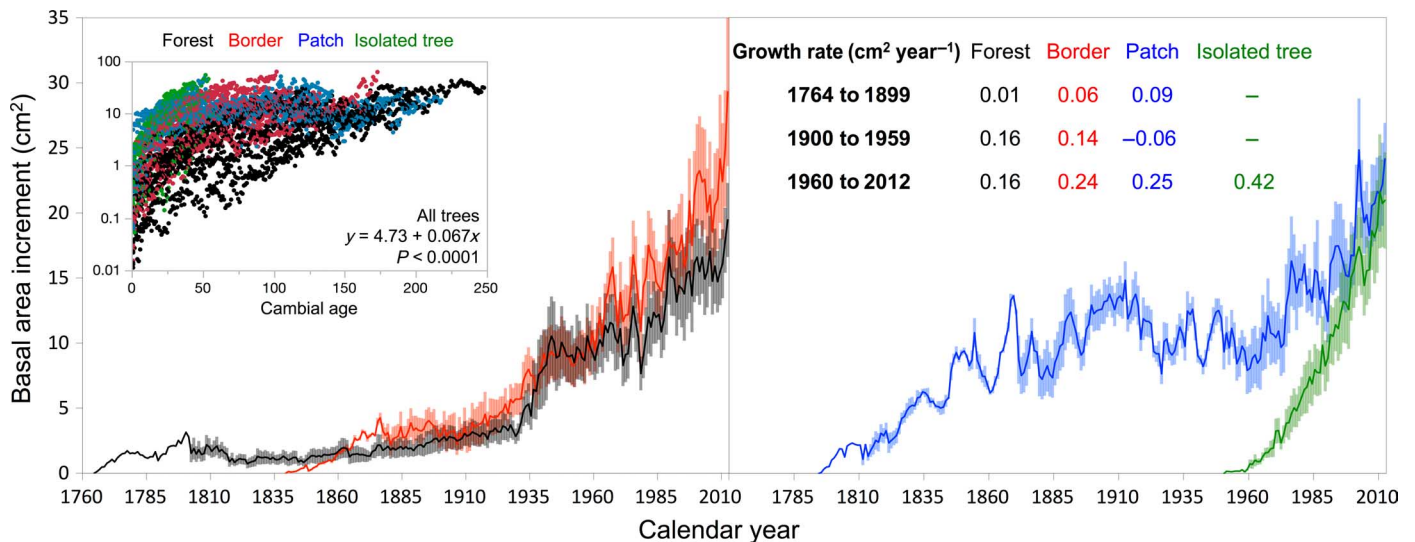

Fig. 2. Basal area increment. Main curves: Average growth of trees sampled in old growth forests (black), forest border (red), forest patches (blue), and isolated trees (green). Shaded areas represent SEs. Inner left: Relationship between BAI and age (log-transformed axis) indicating that increased growth is partly, but not entirely (Fig. 3), influenced by ontogeny. Inner right: Average growth rates from the slopes of linear regressions ($P < 0.001$) of BAI over time (table S4).

BAI using fixed diameters further corroborated that tree growth increased across the gradient regardless of ontogenic effects (fig. S3). Generally, stable late-to-early wood growth ratios (fig. S4) and a stronger relationship between BAI and annual average temperatures than with seasonal temperature fluctuations (table S3) indicate that factors other than changes in the length of the growing season, as considered below, may be responsible for rapid increases in tree growth.

Carbon isotopes

Changes in tree ring carbon isotope ratios over time are consistent with CO_2 stimulation of photosynthesis. We observed a significant decline in tree ring $\delta^{13}C$ values following atmospheric CO_2 enrichment (fig. S5). Atmospheric $\delta^{13}C$ values have been depleted because of fossil carbon emissions (fig. S6) affecting wood isotope composition of all trees, regardless of their age (fig. S7). For this reason, the analysis of carbon isotope ratios must consider changes in atmosphere-to-plant
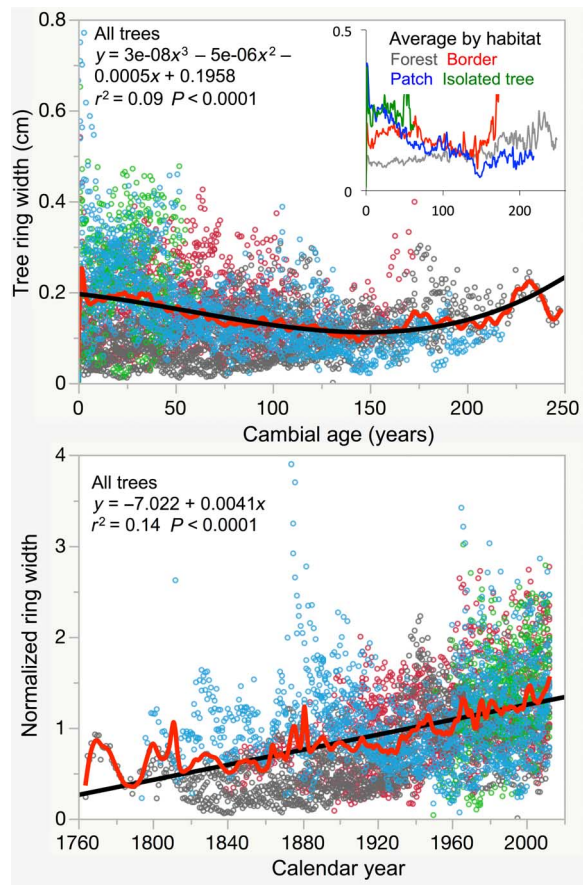
Fig. 3. Regional curve standardization. Top: Ring widths aligned to cambial age, showing that growth rates are influenced by the ontogeny (size/age) of the tree. Bottom: Ring widths divided by the average value at each cambial age (that is, ring width index), showing increasing growth even when normalized by ontogeny.

$^{13}CO_2$ discrimination ($\Delta^{13}C$). A sharp decline in $\Delta^{13}C$ was observed in the early 1900s, marking the beginning of a continuous increase in intrinsic water-use efficiency (iWUE), that is, the ratio between the amount of CO_2 fixed per unit of water lost through transpiration. Increasing iWUE was strongly associated with rising temperatures and CO_2 concentration (tables S2 and S3). Since the 1960s, measured iWUE values were at the same level or lower than those expected under constant intercellular (C_i) to ambient (C_a) CO_2 levels (gray triangles; Fig. 4), with notable differences observed across habitats. Trees growing in the forest interior and patches had lower iWUE than those growing in the forest border or isolated in the grassland. The largest differences in iWUE among habitats were observed between trees in forest patches and forest border ($\sim$20 μmol mol^{-1}), but the overall increase in iWUE across the gradient was severalfold greater than habitat differences.

Oxygen isotopes
Consistent with changes in iWUE, an increasing trend in tree ring $\delta^{18}O$ values was observed for all trees across the gradient (Fig. 4). During the recent phase of tree growth acceleration, wood $\delta^{18}O$ values increased between 3 and 5‰, a response that was positively

associated with atmospheric CO_2 and temperature, and negatively associated with precipitation (table S3). The strength of these relationships indicates that changes in leaf gas exchange (that is, increased iWUE) and, possibly, a warming-induced shift in local hydrology (that is, enrichment of soil water $\delta^{18}O$ values) rather than precipitation amount were the main factors driving the trend in tree ring oxygen isotopes. On the basis of the parallel increases in tree growth and iWUE, it can be inferred that photosynthetic stimulation could more than compensate for any declines in stomatal conductance, which is consistent with previous observations of warming- and CO_2-induced tree growth acceleration.

Nitrogen isotopes and C/N ratios
Tree ring $\delta^{15}N$ values varied significantly across the vegetation gradient (table S2), with no clear trends observed over time (Fig. 5). Wood $\delta^{15}N$ values of forest trees were always below atmospheric levels (0‰), whereas values of wood $\delta^{15}N$ beyond the forest border ranged between 1 and 5‰, with the highest values observed for isolated trees. These results indicate different sources of soil nitrogen across the gradient, but the role of soils in modulating tree growth rates can be better understood when trends in wood nitrogen concentrations are considered. Wood carbon–to–nitrogen (C/N) ratios were highest (>750) in the forest interior ~100 years ago and isolated trees during their initial establishment, implying strong nitrogen limitation. Concurrently with the recent surge in growth, all trees experienced linear declines in C/N, converging to <400 in recent years, which indicates a recent increase in soil nitrogen availability.

DISCUSSION

Increasing tree growth and forest expansion
At the upper limit of alpine forest distribution in eastern Tibet, we documented a strong acceleration of tree growth in recent years. Growth rates of dominant *A. faxoniana* trees were positively associated with rising temperatures and atmospheric CO_2 levels, showing a response similar to those observed in other alpine ecotones (*14–16*). Here, the trajectory of BAI since ~1760 can be divided into three main phases: (i) a phase characterized by very low growth before the early 1900s, (ii) a phase characterized by a steady increase in growth since the early 1900s, (iii) and a phase characterized by sharp surges in growth in the 1930s and 1960s. During the past few decades, annual growth increments were 5 to 10 times higher than those documented in the 19th century, with the relative ages of trees in different habitats suggesting that tree growth acceleration was associated with the establishment of trees in grasslands. This observation is consistent with our hypothesis and the colonization strategy of this species. *A. faxoniana* trees can live longer than 350 years and form dense forest stands at altitudes ranging from 1500 to 3900 m above sea level (asl), where they become dominant through pulses of establishment when environmental conditions are favorable (*18, 19*).

Tree growth acceleration was ubiquitous in different habitats; however, some differences in the timing and magnitude of growth response across these habitats imply differences in resource availabilities (discussed below). Small/young trees recently established in the grassland have grown faster (>2.5-fold) than large/old trees in the forest interior. In forest patches, the first phase of growth increase preceded the response observed in other portions of the gradient,
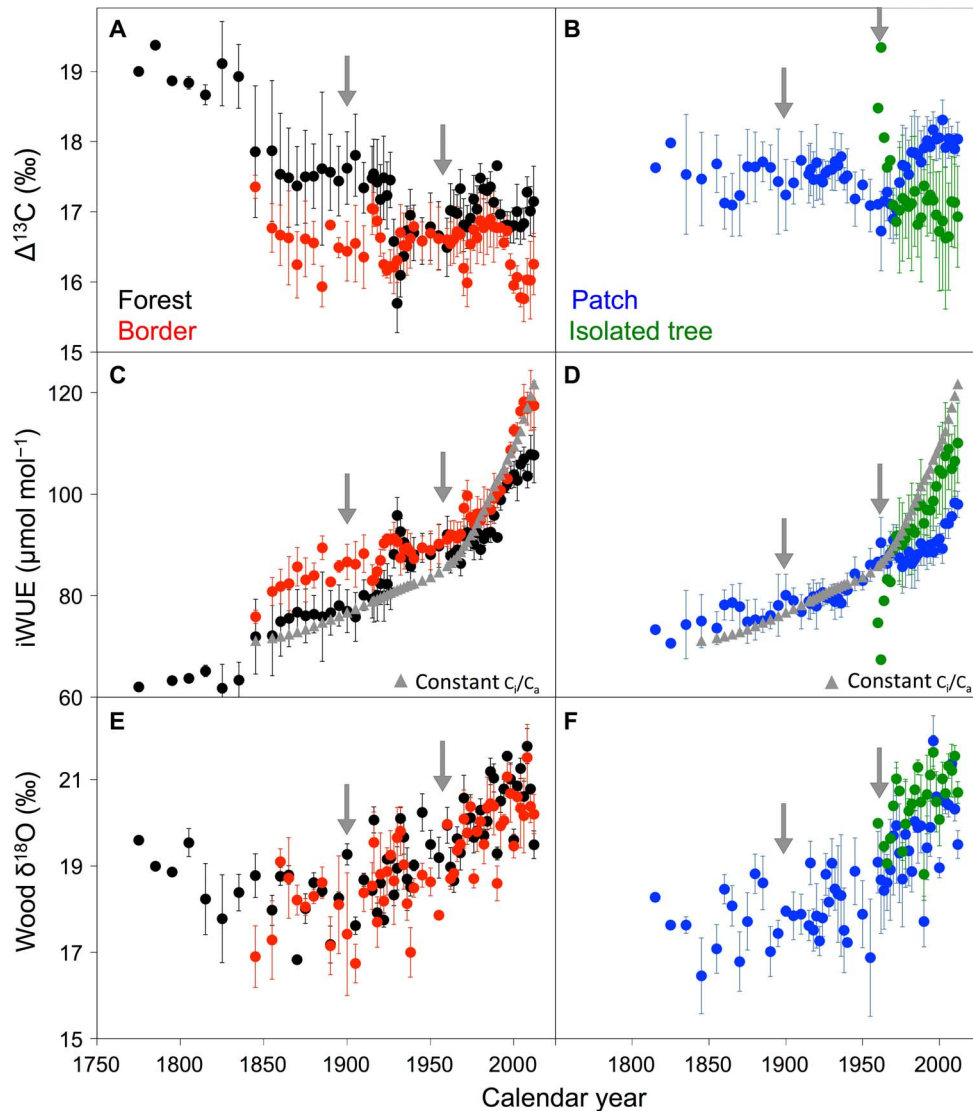
Fig. 4. Carbon and oxygen isotopes. (**A** and **B**) Atmosphere-to-wood carbon isotope fractionation ($\Delta^{13}C$) showing significant interactions between habitat and CO_2 effects. (**C** and **D**) iWUE alongside a modeled baseline of constant C_i/C_a (gray triangles), below which measured values suggest a relatively weaker stomatal control of gas exchange, attributed to increasing water availability. (**E** and **F**) Wood $\delta^{18}O$ values reflecting changes in plant water source, attributed to thawing permafrost. Error bars represent SEs. Arrows show periods of tree growth acceleration.

possibly as a result of plant community diversification (table S4) and associated plant-microbe interactions (20), known to facilitate forest expansion through patch formation in other ecotonal regions (21, 22). During the recent phase of growth acceleration (since 1960), trees have grown faster (~60%) in forest patches and forest border than in the forest interior. Despite these differences, BAI and normalized ring width trajectories, which control for ontogenic effects (23, 24), show increasing growth rates for all trees across the gradient.

Carbon isotopes: The effect of atmospheric CO_2
Consistent with a scenario of CO_2 fertilization (15, 16), we identified parallel increases in iWUE and BAI for all trees across the gradient, but significant interactions were observed between habitat and CO_2 effects on tree growth. Habitat effects are reflected on divergent $\Delta^{13}C$ trajectories, which indicate higher iWUE in the forest border

and isolated trees than in the forest interior or forest patches. These differences are consistent with the expectation of lower insolation and higher moisture under closed canopies, where iWUE values measured since 1960 show a relatively weaker stomatal regulation of leaf gas exchange relative to a baseline of constant C_i/C_a (Fig. 4). Habitat differences could also have resulted from gradients in soil nutrient availability (9, 13), which would have favored a stronger photosynthetic response to elevated CO_2 at and beyond the forest border, where competition for nutrients is lower. Consistent with this interpretation, trees sampled in open areas have grown faster than trees in the forest interior, but the overall increase in iWUE (and growth)—observed for all trees in response to rising temperatures and CO_2 levels—was much greater than differences between habitats. Moreover, the increase in iWUE over time across habitats can be considered a moderate response compared to those observed, for example, under drought
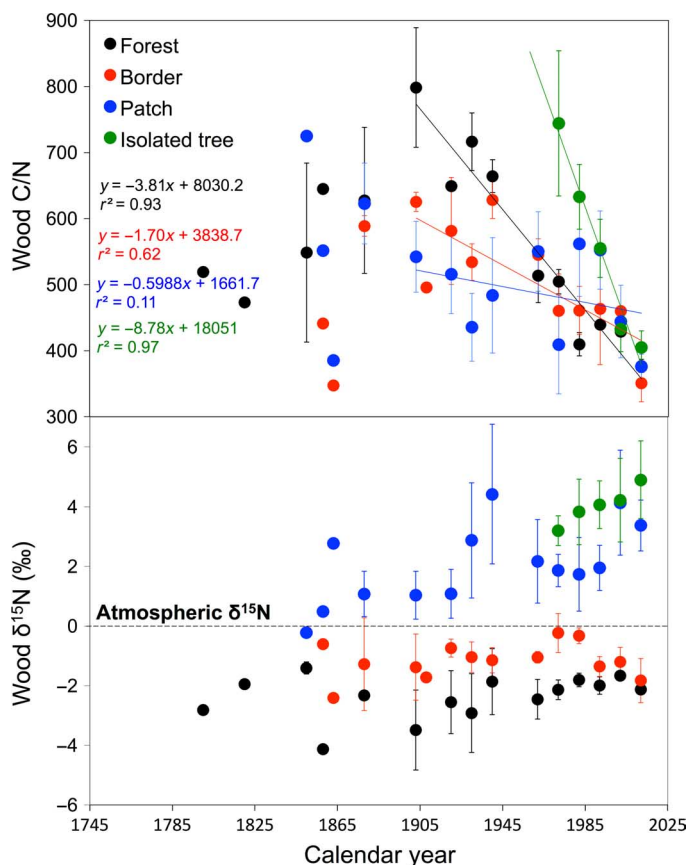
Fig. 5. Nitrogen isotopes and C/N ratios. Regression lines represent changes occurred since 1900 at different habitats. Error bars represent SEs.

stress or strong stomatal regulation needed to maintain C_i constant as C_a rises (25, 26). Furthermore, given that iWUE was not influenced by fluctuations in precipitation and that increasing tree growth prevailed across habitats, it is apparent that increasing efficiency (in this case) was driven by photosynthetic stimulation rather than declining stomatal conductance to conserve water.

Oxygen isotopes: The effect of soil water availability

Changes in wood $\delta^{18}O$ values over time suggest that recent permafrost thawing contributed to increasing tree growth and forest expansion. The trajectory of tree ring $\delta^{18}O$ values mirror trends in BAI and iWUE, indicating a positive photosynthetic response to rising CO_2 levels (27), accompanied by increasing $\delta^{18}O$ values of plant water source. Following the general relationship between air temperature and $\delta^{18}O$ signatures of precipitation ($\delta^{18}O = 0.69$temp $- 13.6$) (28), the observed increase in wood $\delta^{18}O$ values suggest a ~5°C warming, which is several times higher than the actual temperature increase registered at the site (fig. S5). Therefore, warming-induced changes in isotopic signatures of precipitation water cannot explain the observed increase in tree ring $\delta^{18}O$ values, which, combined with the weak relationship between wood $\delta^{18}O$ values and precipitation amount (table S3), suggests a recent change in soil hydrology. With a few exceptions—for example, water uptake by salt-excluding species in saline environments (29)—there is no isotopic discrimination during plant water uptake (30), and, as a result, tree ring $\delta^{18}O$ values

reflect those of soil water. As in many alpine ecosystems, soils at the study site are cryogenic and can be classified into two main groups: cryic (with mean annual temperature below 8°C) and pergelic (with temperatures below 0°C). The latter category includes permafrosts, which experience enhanced cycling of water, carbon, and nutrients under warming (31). Currently, gelic materials are found within 100 cm from the soil surface and, on the basis of the registered temperature increase (fig. S5), it can be inferred that permafrost thawing at the site began in the 1960s, coinciding with tree growth acceleration and establishment into grasslands (as well as with a shift in iWUE from higher to lower values relative to a baseline of constant C_i/C_a). When meltwater infiltrates the frozen organic layer, it leads to saturation in the pore spaces, mixing enriched and unenriched water pools. As thawing progresses, the value of soil water $\delta^{18}O$ gradually increases at rates that could explain the trend observed in tree rings (32). A shift from pergelic to cryic conditions also permits greater tree root development and nutrient uptake (33), favoring tree growth and forest expansion. However, it is important to note that our $\delta^{18}O$ results were obtained from bulk wood and—although the magnitude and direction of $\delta^{18}O$ values of bulk plant materials is expected to vary in concert with those measured in specific compounds, such as cellulose (34)—wood $\delta^{18}O$ values are often considered less sensitive than compound-specific records of hydrological change (35, 36).

Nitrogen isotopes and wood C/N: The effect of nutrient availability

The role of permafrost thawing in accelerating tree growth is further supported by wood nitrogen content, because permafrost thawing can increase both water and nutrient availability to trees. We found evidence of strong nitrogen limitation in the forest interior ~100 years ago (C/N >750) and in isolated trees during their initial development. In recent decades, wood nitrogen content increased significantly (C/N <400), regardless of tree age or habitat. This finding indicates a marked change in nitrogen availability, which coincides with the recent phase of tree growth acceleration, and would have allowed a sustained positive response to elevated CO_2. This interpretation is consistent with recent studies of European forests, where growth acceleration (also accentuated in 1960s) was attributed to increasing nitrogen deposition (37). In contrast with European forests, eastern Tibet is distant from industrial centers and receives very low amounts of nitrogen via atmospheric deposition (<0.5 g N m^{-2} year^{-1}) (38). Moreover, if changes in C/N ratios had been caused by atmospheric deposition, then this would have affected the isotopic composition of trees across the entire gradient. Instead, contrasting $\delta^{15}N$ signals indicate different sources of nitrogen in different portions of the gradient. Evidently, the analysis of tree ring $\delta^{15}N$ values is complicated by the fact that trees can recover nitrogen from dying cells during the conversion from sapwood to heartwood (39). Nevertheless, $\delta^{15}N$ signals remain stable after heartwood formation, thus providing an indication of changes in nitrogen source (40, 41). Symbiotic interactions lead to low $\delta^{15}N$ values because nitrification supplies plants with ^{15}N-depleted amino acids that are near the atmospheric signature. Here, tree ring $\delta^{15}N$ values indicate a greater contribution of nitrogen-fixing organisms in forests and a predominant contribution of ^{15}N-enriched organic forms in patches and isolated trees (20, 33, 42), which could explain the differences we observed in tree growth patterns and iWUE across habitats. Alternatively, differences in tree ring $\delta^{15}N$ values could be the result of

Silva et al. Sci. Adv. 2016;2:e1501302   31 August 2016

5 of 8

increased rooting depth with increasing tree size (43), but we did not find a significant effect of tree size on $\delta^{15}N$ values. Moreover, changes in root depth cannot explain the decline in C/N ratios across the gradient, which is consistent with a scenario of nitrogen inputs from thawing permafrost.

Final considerations

By combining dendrochronological and isotopic measurements, we showed that recent changes in climate and atmospheric composition have had a strong positive effect on tree growth attributed to direct and indirect drivers (that is, photosynthetic stimulation and resources released from permafrost thawing). Multiple lines of evidence point to a connection between the physiological performance of dominant trees and shifts in forest distribution, which is consistent with expected responses for alpine ecosystems, but contrasts with recent accounts of growth decline in forests dominated by trees of the same genus (Abies) and at similar altitudes in other parts of the world (8, 44). The eastern Tibetan Plateau has been described as a stable region where "climatically induced ecological thresholds have not yet been crossed" (45). This assessment, which is based on palynological records of the past 600 years, suggests that the recent surge in tree growth and expansion of forests reported here have yet to be manifested at broader scales. Notably, the response of dominant trees is not necessarily representative of broad trends in forest distribution. For example, it has been argued that "the world's most frequently applied sampling design," that is, the dendrochronological analysis of dominant trees, can lead to biases in growth trends in excess of 200% relative to nondominant trees (46). Nevertheless, our analysis included trees of various ages and sizes in different habitats, which minimizes the chance of a systematic bias (23, 24, 47). We suspect that discrepant site-specific responses to changes in climate and atmospheric composition can be explained by differences in edaphic properties. Accordingly, we anticipate that consideration of soil-plant-atmosphere interactions in future studies will improve our ability to predict and manage shifts in productivity and distribution of forest ecosystems.

MATERIALS AND METHODS

Study site

The study site is located near the Waqie Grasslands National Park (33°03.858′N and 102°48.847′E), in a remote part of the Sichuan Province, China (Fig. 1, A and B). It represents a typical forest-grassland ecotone located at ~3650 m asl in the eastern side of the Tibetan Plateau. The regional climate can be characterized as a typical plateau continental climate with high solar radiation, short-cool summers (mean, July; maximum/minimum, 14.6°/7.6°C), and long-cold winters (mean, January; maximum/minimum, −3.0°/−17.2°C). A short plant-growing season is determined by the influence of the southeastern monsoon, and the winter climate systems is dominated by cold air masses originating from Siberia. Approximately 80% of the annual precipitation is distributed during the growing season, which begins at the end of April or early May and ends in late September. According to data recorded at the Hongyuan County meteorological station since 1960 (fig. S3), the average annual temperature has increased significantly over

the past decades from 0.5° to 1.5°C before the 1980s (with few exceptions) to 2° to 2.8°C in the 2000s. The average annual precipitation ranges from 50 to 80 cm with no systematic change observed over time.

Vegetation gradient

We studied a natural vegetation mosaic with readily distinguishable transitions between old growth forests and grasslands. We used a systematic sampling design with five transects (fig. S1) to perform a census of the vegetation (table S4) at the end of the growing season (October 2012). Along each transect, ten 100-m^2 plots were used to characterize each portion of the gradient: forest interior, forest border, large patches (>15-m diameter), and isolated trees. At each plot, two cores were taken (~1.3 m above ground level) from the largest A. faxoniana using a wood Pressler borer. We sampled 10 trees in the forest interior, 10 isolated trees, 11 trees at the border, and 11 trees in forest patches at similar altitudes and in north-facing slopes to avoid possible confounding effects from grazing—nomadic herders use warmer south-facing slopes as pasture. Throughout the gradient, the soil was a typical alpine Cryogenic Cambisol-Cyumbrept (Gelisols in the U.S. soil classification system), having gelic materials within less than 100 cm of the soil surface and consisting of 19% clay, 66% silt, and 15% sand (pH 5.0 to 6.0) [0- to 10-cm depth; 1:2.5, soil/water (v/v)].

Growth measurements

We used measurements of tree ring width from healthy dominant trees of cylindrical stem to calculate BAI. This metric is closely related to annual aboveground productivity and unlike ring width, which tends to decline with age, can reliably detect changes in growth long after trees reach maturity (8, 23). To estimate BAIs over time, wood cores were mounted, sanded, polished, scanned, and cross-dated, and ring widths were measured using the software WinDENDRO (Regent Instruments Inc.). Measurements of trees growing in the forest and grasslands are presented separately to represent the gradient in competitive environment and time of establishment. Assuming that annual increments were uniform along each ring, BAI was calculated as follows

$$BAI = \pi * (R_t^2 - R_{t-1}^2) \tag{1}$$

where R is the tree radius and t is the year of tree ring formation.

Isotopic measurements

Growth curves were used to guide subsampling within wood cores for isotopic analysis. Wood cores from the 12 trees best correlated with the average chronology were destructively processed for the determination of $\delta^{13}C$, $\delta^{18}O$, $\delta^{15}N$, and C/N ratios. We measured the isotopic composition of single or multiple (pooled) tree rings for each individual tree. To determine $\delta^{13}C$ and $\delta^{18}O$ shifts, annual rings were used during periods of high tree growth variation, and 3- to 5-year pooled rings were used to characterize periods of steady growth. Because of low nitrogen concentrations, $\delta^{15}N$ determination always involved the combination of three to five rings, in which total nitrogen concentration was also measured. In all cases, pooled samples were obtained from individual tree cores and averages and SEs were determined using data from multiple trees. Isotopic analyses were

performed at the Stable Isotope Facility of the University of California, Davis and are expressed as follows

$$\delta\,(\text{\textperthousand})\,=\,(R_{\text{sample}}/R_{\text{standard}}-1)\,*\,1000 \qquad (2)$$

where R_{sample} and R_{standard} are the abundance ratios of a given sample and the standard, namely, the Vienna Pee Dee Belemnite formation for $\delta^{13}C$, the Vienna Standard Mean Ocean Water for $\delta^{18}O$, and atmospheric $\delta^{15}N$ values.

The interpretation of carbon isotopes followed derivations necessary to correct for variation in atmospheric $\delta^{13}C$ (48, 49)

$$\Delta^{13}C\,=\,(\delta^{13}C_{\text{air}}-\delta^{13}C_{\text{plant}})/(1\,+\,\delta^{13}C_{\text{air}}/\,1000) \qquad (3)$$

where $\Delta^{13}C$ represents the discrimination against ^{13}C, $\delta^{13}C_{\text{air}}$ is the carbon isotope ratio of air (the source), and $\delta^{13}C_{\text{plant}}$ is the carbon isotope ratio of the product (plant biomass).

$$C_{\text{i}}\,=\,C_{\text{a}}\,*\,(\Delta^{13}C-a)\,/\,(b-a) \qquad (4)$$

where a is the discrimination against $^{13}CO_2$ during diffusion through the stomata in the gaseous phase (4.4‰), and b is the net discrimination due to carboxylation (27‰).

$$\text{iWUE}\,=\,A/g = C_{\text{a}}\,*\,[\,1\,-\,(C_{\text{i}}/C_{\text{a}})\,]\,*\,0.625 \qquad (5)$$

where A is net carboxylation, g is the leaf stomatal conductance, and 0.625 is the relation between conductance for CO_2 molecules and water vapor.

Measured iWUE was compared with modeled values (gray triangles; Fig. 4) used to delineate a theoretical baseline of constant $C_{\text{i}}/C_{\text{a}}$ accounting for changes in CO_2 partial pressure over time and across altitudinal gradients (50). The interpretation of iWUE results was assisted by independent measurements of oxygen and nitrogen isotopes (41).

Statistical analysis

To summarize the strength and direction of relationships between environmental and tree ring variables, we used pairwise correlations applied to the entire data set (table S3). A regional curve standardization was performed using ring widths aligned to cambial age to remove ontogenic effects and assess the consistency of growth trends over time. Ring widths of all trees were divided by the average growth for each cambial age, and the resulting normalized data were plotted in relation to calendar year (23). To evaluate the effect of tree size, growth rates were compared using fixed diameters plotted in relation to calendar year using rings formed when all trees reached the target size (24). When appropriate, least-squares regressions were used to describe trends in growth and wood chemical composition at different portions of the gradient. In all cases, adjusted coefficients of determination (r^2) and probabilities were reported. In addition, two sets of mixed-effects models were used to further analyze the data (tables S5 and S6). The first encompassed the entire chronology, examining changes in growth since 1760. The second targeted the period since meteorological record keeping began (1960). Both models included tree identity and/or calendar year as random effects,

with random intercepts and slopes centered at the fixed-effects (51). Alternative mixed-effects models were tested using different combinations of explanatory variables (table S2). The most parsimonious model was selected on the basis of Akaike's information criterion (AIC) defined as $\text{AIC} = -2L + 2K$, where L is the maximum log-likelihood of the model, and K is the number of parameters in the model (52). BAI values were log-transformed, and isotopic data were normalized—that is, divided by the historical average—before analysis. Transformations and number of measurements used in each analysis are shown in the Supplementary Materials. Untransformed values and associated SEs are shown in the main text. In all cases, significance levels were set at $P < 0.05$.

SUPPLEMENTARY MATERIALS

Supplementary material for this article is available at http://advances.sciencemag.org/cgi/content/full/2/8/e1501302/DC1

fig. S1. Sketch of sampling design, showing five transects distributed across a typical alpine forest grassland transition.
fig. S2. Relationship between tree age and size at the time of sampling ($y = 0.06x + 10.08$; $r^2 = 0.41$; $P < 0.01$).
fig. S3. Normalized tree ring widths and basal area increments plotted over time using individual measurements of all rings formed when trees reached two fixed diameters (10 to 11 and 30 to 31 cm).
fig. S4. Late to early wood growth indicating stable seasonal growth patterns in recent decades.
fig. S5. Wood and atmospheric carbon isotope composition.
fig. S6. Meteorological data and atmospheric CO_2.
fig. S7. Relationship between tree age and wood carbon, oxygen, and nitrogen stable isotope ratios (green, isolated trees; blue, forest patches; red, forest border; black, forest interior).
table S1. Summary of mixed-effect model examining changes in tree growth over time at different portions of the vegetation gradient.
table S2. Summary of mixed-effect models relating environmental factors and isotopic proxies of physiological performance during the recent tree growth acceleration phase (since 1960).
table S3. Pairwise correlations of untransformed variables performed using the entire data set.
table S4. Linear basal area increment (BAI) trends used to estimate growth rates, summarized in Fig. 2 by habitat and time periods.
table S5. Floristic composition and ecological characteristics of the dominant tree species.
table S6. An information-theoretic approach to evaluate multiple mixed-effect models and derive predictions that best represent the documented changes in tree growth.
table S7. Structure of mixed-effect models used in this study.

REFERENCES AND NOTES

1. N. B. Grimm, F. Stuart Chapin III, B. Bierwagen, P. Gonzalez, P. M. Groffman, Y. Luo, F. Melton, K. Nadelhoffer, A. Pairis, P. A. Raymond, J. Schimel, C. E. Williamson, The impacts of climate change on ecosystem structure and function. *Front. Ecol. Environ.* **11**, 474–482 (2013).
2. L. Silva, M. Anand, Historical links and new frontiers in the study of forest-atmosphere interactions. *Community Ecol.* **14**, 208–218 (2013).
3. M. Benito-Garzón, P. W. Leadley, J. F. Fernández-Manjarrés, Assessing global biome exposure to climate change through the Holocene–Anthropocene transition. *Glob. Ecol. Biogeogr.* **23**, 235–244 (2014).
4. E. A. Ainsworth, S. P. Long, What have we learned from 15 years of free-air CO_2 enrichment (FACE)? A meta-analytic review of the responses of photosynthesis, canopy properties and plant production to rising CO_2. *New Phytol.* **165**, 351–371 (2005).
5. J. Peñuelas, J. G. Canadell, R. Ogaya, Increased water-use efficiency during the 20th century did not translate into enhanced tree growth. *Glob. Ecol. Biogeogr.* **20**, 597–608 (2011).
6. P. J. van Mantgem, N. L. Stephenson, J. C. Byrne, L. D. Daniels, J. F. Franklin, P. Z. Fulé, M. E. Harmon, A. J. Larson, J. M. Smith, A. H. Taylor, T. T. Veblen, Widespread increase of tree mortality rates in the western United States. *Science* **323**, 521–524 (2009).
7. Z. Gedalof, A. A. Berg, Tree ring evidence for limited direct CO_2 fertilization of forests over the 20th century. *Global Biogeochem. Cycles* **24**, GB3027 (2010).
8. A. Gómez-Guerrero, L. C. R. Silva, M. Barrera-Reyes, B. Kishchuk, A. Velázquez-Martínez, T. Martínez-Trinidad, F. O. Plascencia-Escalante, W. R. Horwath, Growth decline and divergent tree ring isotopic composition ($\delta^{13}C$ and $\delta^{18}O$) contradict predictions of CO_2 stimulation in high altitudinal forests. *Glob. Chang. Biol.* **19**, 1748–1758 (2013).

9. M. Fernández-Martínez, S. Vicca, I. A. Janssens, J. Sardans, S. Luyssaert, M. Campioli, F. S. Chapin III, P. Ciais, Y. Malhi, M. Obersteiner, D. Papale, S. L. Piao, M. Reichstein, F. Rodà, J. Peñuelas, Nutrient availability as the key regulator of global forest carbon balance. *Nat. Clim. Chang.* 4, 471–476 (2014).

10. R. Oren, D. S. Ellsworth, K. H. Johnsen, N. Phillips, B. E. Ewers, C. Maier, K. V. R. Schäfer, H. McCarthy, G. Hendrey, S. G. McNulty, G. G. Katul, Soil fertility limits carbon sequestration by forest ecosystems in a CO_2-enriched atmosphere. *Nature* 411, 469–472 (2001).

11. L. C. R. Silva, A. Salamanca-Jimenez, T. A. Doane, W. R. Horwath, Carbon dioxide level and form of soil nitrogen regulate assimilation of atmospheric ammonia in young trees. *Sci. Rep.* 5, 13141 (2015).

12. A. J. Bloom, J. S. Rubio Asensio, L. Randall, S. Rachmilevitch, A. B. Cousins, E. A. Carlisle, CO_2 enrichment inhibits shoot nitrate assimilation in C_3 but not C_4 plants and slows growth under nitrate in C_3 plants. *Ecology* 93, 355–367 (2012).

13. A. C. Finzi, D. J. P. Moore, E. H. DeLucia, J. Lichter, K. S. Hofmockel, R. B. Jackson, H.-S. Kim, R. Matamala, H. R. McCarthy, R. Oren, J. S. Pippen, W. H. Schlesinger, Progressive nitrogen limitation of ecosystem processes under elevated CO_2 in a warm-temperate forest. *Ecology* 87, 15–25 (2006).

14. G. C. Jacoby, R. D. D'Arrigo, T. Davaajamts, Mongolian tree rings and 20th-century warming. *Science* 273, 771–773 (1996).

15. C. Körner, *Alpine Treelines:Functional Ecology of the Global High Elevation Tree Limits* (Springer, Basel, 2012), p. 220.

16. M. W. Salzer, M. K. Hughes, A. G. Bunn, K. F. Kipfmueller Recent unprecedented tree-ring growth in bristlecone pine at the highest elevations and possible causes. *Proc. Natl. Acad. Sci. U.S.A.* 106, 20348–20353 (2009).

17. L. C. R. Silva, From air to land: Understanding water resources through plant-based multidisciplinary research. *Trends Plant Sci.* 20, 399–401 (2015).

18. A. H. Taylor, J. S. Wei, Z. L. Jun, L. C. Ping, M. C. Jin, H. Jinyan, Regeneration patterns and tree species coexistence in old-growth *Abies–Picea* forests in southwestern China. *For. Ecol. Manage.* 223, 303–317 (2006).

19. K. Takahashi, Regeneration and coexistence of two subalpine conifer species in relation to dwarf bamboo in the understorey. *J. Veg. Sci.* 8, 529–536 (1997).

20. H. Lambers, C. Mougel, B. Jaillard, P. Hinsinger, Plant-microbe-soil interactions in the rhizosphere: An evolutionary perspective. *Plant Soil* 321, 83–115 (2009).

21. R. G. Pearson, Climate change and the migration capacity of species. *Trends Ecol. Evol.* 21, 111–113 (2006).

22. L. C. R. Silva, M. Anand Mechanisms of Araucaria (Atlantic) forest expansion into southern Brazilian grasslands. *Ecosystems* 14, 1354–1371 (2011).

23. R. L. Peters, P. Groenendijk, M. Vlam, P. A. Zuidema, Detecting long-term growth trends using tree rings: A critical evaluation of methods. *Glob. Chang. Biol.* 21, 2040–2054 (2015).

24. P. van der Sleen, P. Groenendijk, M. Vlam, N. P. R. Anten, A. Boom, F. Bongers, T. L. Pons, G. Terburg, P. A. Zuidema, No growth stimulation of tropical trees by 150 years of CO_2 fertilization but water-use efficiency increased. *Nat. Geosci.* 8, 24–28 (2015).

25. M. Saurer, R. T. W. Siegwolf, F. H. Schweingruber, Carbon isotope discrimination indicates improving water-use efficiency of trees in northern Eurasia over the last 100 years. *Glob. Chang. Biol.* 10, 2109–2120 (2004).

26. J. C. Linares, J. Camarero, From pattern to process: Linking intrinsic water-use efficiency to drought-induced forest decline. *Glob. Chang. Biol.* 18, 1000–1015 (2012).

27. Y. Scheidegger, M. Saurer, M. Bahn, R. Siegwolf, Linking stable oxygen and carbon isotopes with stomatal conductance and photosynthetic capacity: A conceptual model. *Oecologia* 125, 350–357 (2000).

28. W. Dansgaard, Stable isotopes in precipitation. *Tellus* 16, 436–468 (1964).

29. P. Z. Ellsworth, D. G. Williams, Hydrogen isotope fractionation during water uptake by woody xerophytes. *Plant Soil* 291, 93–107 (2007).

30. M. M. Barbour, Stable oxygen isotope composition of plant tissue: A review. *Funct. Plant Biol.* 34, 83–94 (2007).

31. J. K. Jansson, N. Taş, The microbial ecology of permafrost. *Nat. Rev. Microbiol.* 12, 414–425 (2014).

32. S. K. Carey, W. L. Quinton, Evaluating snowmelt runoff generation in a discontinuous permafrost catchment using stable isotope, hydrochemical and hydrometric data. *Nord. Hydrol.* 35, 309–324 (2004).

33. C. Shi, L. C. R. Silva, H. Zhang, Q. Zheng, B. Xiao, N. Wu, G. Sun, Climate warming alters nitrogen dynamics and total non-structural carbohydrate accumulations of perennial herbs of distinctive functional groups during the plant senescence in autumn in an alpine meadow of the Tibetan Plateau, China. *Agric. For. Meteorol.* 200, 21–29 (2015).

34. L. C. R. Silva, G. Pedroso, T. A. Doane, F. N. D. Mukome, W. Horwath, Beyond the cellulose: Oxygen isotope composition of plant lipids as a proxy for terrestrial water balance. *Geochem. Persp. Lett.* 1, 33–42 (2015).

35. A. Gessler, J. P. Ferrio, R. Hommel, K. Treydte, R. A. Werner, R. K. Monson, Stable isotopes in tree rings: Towards a mechanistic understanding of isotope fractionation and mixing processes from the leaves to the wood. *Tree Physiol.* 34, 796–818 (2014).

36. L. S. L. O'Reilly Sternberg, Oxygen stable isotope ratios of tree-ring cellulose: The next phase of understanding. *New Phytol.* 181, 553–562 (2009).

37. H. Pretzsch, P. Biber, G. Schütze, E. Uhl, T. Rötzer, Forest stand growth dynamics in Central Europe have accelerated since 1870. *Nat. Commun.* 5, 4967 (2014).

38. C. Jiang, G. Yu, H. Fang, G. Cao, Y. Li, Short-term effect of increasing nitrogen deposition on CO_2, CH_4 and N_2O fluxes in an alpine meadow on the Qinghai-Tibetan Plateau, China. *Atmos. Environ.* 44, 2920–2926 (2010).

39. P. Meerts, Mineral nutrient concentrations in sapwood and heartwood: A literature review. *Ann. For. Sci.* 59, 713–722 (2002).

40. M. Saurer, P. Cherubini, M. Ammann, B. De Cinti, R. Siegwolf, First detection of nitrogen from NO_x in tree rings: A $^{15}N/^{14}N$ study near a motorway. *Atmos. Environ.* 38, 2779–2787 (2004).

41. T. M. Maxwell, L. C. R. Silva, W. R. Horwath, Using multielement isotopic analysis to decipher drought impacts and adaptive management in ancient agricultural systems. *Proc. Natl. Acad. Sci. U.S.A.* 111, E4807–E4808 (2014).

42. Z. Wang, L. C. R. Silva, G. Sun, P. Luo, C. Mou, W. R. Horwath, Quantifying the impact of drought on soil-plant interactions: A seasonal analysis of biotic and abiotic controls of carbon and nutrient dynamics in high-altitudinal grasslands. *Plant Soil* 389, 59–71 (2014).

43. E. A. Hobbie, A. P. Ouimette, Controls of nitrogen isotope patterns in soil profiles. *Biogeochemistry* 95, 355–371 (2009).

44. L. C. R. Silva, A. Gómez-Guerrero, T. A. Doane, W. R. Horwath, Isotopic and nutritional evidence for species- and site-specific responses to N deposition and rising atmospheric CO_2 in temperate forests. *J. Geophys. Res. Biogeosci.* 120, 1110–1123 (2015).

45. J. Wischnewski, U. Herzschuh, K. M. Rühland, A. Bräuning, S. Mischke, J. P. Smol, L. Wang, Recent ecological responses to climate variability and human impacts in the Nianbaoyeze Mountains (eastern Tibetan Plateau) inferred from pollen, diatom and tree-ring data. *J. Paleolimnol.* 51, 287–302 (2014).

46. C. Nehrbass-Ahles, F. Babst, S. Klesse, M. Nötzli, O. Bouriaud, R. Neukom, M. Dobbertin, D. Frank, The influence of sampling design on tree-ring-based quantification of forest growth. *Glob. Chang. Biol.* 20, 2867–2885 (2014).

47. R. J. W. Brienen, E. Gloor, P. A. Zuidema, Detecting evidence for CO_2 fertilization from tree ring studies: The potential role of sampling biases. *Global Biogeochem. Cycles* 26, GB1025 (2012).

48. D. McCarroll, N. J. Loader, Stable isotopes in tree rings. *Quat. Sci. Rev.* 23, 771–801 (2004).

49. G. D. Farquhar, J. R. Ehleringer, K. T. Hubick, Carbon isotope discrimination and photosynthesis. *Annu. Rev. Plant. Physiol. Plant. Mol. Biol.* 40, 503–537 (1989).

50. L. C. R. Silva, W. R. Horwath, Explaining global increases in water use efficiency: Why have we overestimated responses to rising atmospheric CO_2 in natural forest ecosystems? *PLOS One* 8, e53089 (2013).

51. A. F. Zuur, E. N. Ieno, N. Walker, A. A. Saveliev, G. M. Smith, *Mixed Effects Models and Extensions in Ecology with R* (Springer, New York, 2009), p. 574.

52. H. Akaike, in *Information Theory and An Extension of the Maximum Likelihood Principle*, E. Parzen, K. Tanabe, G. Kitagawa, Eds. (Springer, New York, 1998), pp. 199–213.